RESEARCH ARTICLE

Magnetic chitosan-zeolite composite as an adsorbent in ultrasound-assisted magnetic solid phase extraction of tetracyclines in water samples

Mpho Charmaine Lefatle[1,2], Lawrence Mzukisi Madikizela[3], Vusumzi Emmanuel Pakade[4] and Philiswa Nosizo Nomngongo[1,2*]

Abstract

An ultrasound-assisted magnetic solid-phase extraction method was developed to pre-concentrate tetracyclines (TCs) in wastewater and river water. The magnetic chitosan-zeolite composite was used as an adsorbent. The morphological and structural properties of the adsorbent were characterised by various analytical techniques. The factors affecting the ultrasound-assisted magnetic solid-phase extraction method were optimised using a central composite design. A high performance liquid chromatography equipped with a photodiode array detector was used to quantify TCs in wastewater and river water samples. Under optimised parameters, the developed analytical approach gave acceptable linearity (LOQ-400 µg L^{-1}) with correlation coefficients exceeding 0.993, while the detection and quantitation limits ranged from 0.05–0.67 and 0.14–2.03 µg L^{-1}, respectively. Attained recoveries were 90–101%, with intraday and interday precision expressed as the relative standard deviation (%RSD) below 5%. Even though the target analytes (tetracycline, oxytetracycline and oxytetracycline) were not detected in environmental samples, the synthesised adsorbent was suitable for the isolation of TCs in a complex matrix resulting in an accurate, precise, rapid and sensitive analytical method.

Keywords Tetracyclines, Response surface methodology, Wastewater, Ultrasound-assisted magnetic solid phase extraction, Environmental monitoring

*Correspondence:
Philiswa Nosizo Nomngongo
pnnomngongo@uj.ac.za
[1] Department of Chemical Sciences, University of Johannesburg, Doornfontein Campus, P.O. Box 17011, Doornfontein 2028, South Africa
[2] Department of Science and Innovation-National Research Foundation South Africa Research Chair Initiative (DSI-NRF SARChI) in Nanotechnology for Water, University of Johannesburg, Doornfontein 2028, South Africa
[3] Institute for Nanotechnology and Water Sustainability, College of Science, Engineering and Technology, University of South Africa, Florida Science Campus, Roodepoort 1710, South Africa
[4] Department of Chemistry, College of Science, Engineering and Technology, University of South Africa, Florida Science Campus, Roodepoort 1710, South Africa

Introduction

Water pollution caused by antibiotics which enter the water resources via the discharge of effluents from agricultural, municipal, and pharmaceutical industries, has become a worldwide environmental concern. Due to their broad spectrum of antimicrobial effects, tetracyclines (TCs) have become one of the most commonly prescribed antibiotics for treating animal and human diseases (Minale et al. 2020). TCs are chemically stable and low biodegradable antibiotics, with 70–90% of the parent compound excreted into the environment via faeces and urine (Xiong et al. 2018; Yan et al. 2020). A continuous uncontrolled discharge of TCs into the environment can potentially develop bacterial resistance to

Lefatle *et al. Journal of Analytical Science and Technology* (2023) 14:28

Page 2 of 15

these antibiotics (Lu et al. 2019). This, in turn, could render antibiotic treatment costly and challenging. Hence, the environmental monitoring of TCs is essential. Environmental monitoring of TCs is mainly conducted with a liquid chromatographic technique after a suitable sample preparation and clean-up step designed for extracting and pre-concentrating target compounds from the environmental samples (Mamani et al. 2009; Önal 2011). The mostly used solid-phase extraction (SPE) method for sample preparation is associated with economic disadvantages due to the single usage of commercially available cartridges packed with various sorbents and high solid waste generation (Madikizela and Chimuka 2017).

Chitosan (Cs) is known for its excellent properties such as biocompatibility, biodegradability, non-toxicity, abundance, bioactivity, biosorption and good adsorption, making it an excellent candidate for water purification and extraction processes (Elsoud and Kady 2019; Feria-Diaz et al. 2018; Qin et al. 2020). Cs is a copolymer made of D-glucosamine and *N*-acetyl-D-glucosamine held together by β-1-4-glycosidic bonds (deAlvarenga 2011). The presence of highly reactive amino and hydroxyl groups in the chitosan molecule increases its adsorption capacity towards contaminants due to the ability to form hydrogen bonds and electrostatic interactions with adsorbates (Siddeeg et al. 2020). The amount of protonated amino groups influences the solubility, biodegradability, reactivity and adsorption of various compounds in the polymeric chain (Lodhi et al. 2014). Despite its excellent properties, chitosan has some disadvantages, including poor mechanical properties, difficulty separating it from water after adsorption, and low specific gravity (Siddeeg et al. 2020). Therefore, to combat these disadvantages, this study proposes mixing chitosan with other materials, such as zeolite, thus improving its overall adsorption performance.

Zeolites (Z) are crystalline aluminosilicates consisting of three-dimensional (3D) microporous structures. Hence, zeolites were considered adsorbents in the present study due to their excellent mechanical and thermal stability, availability in abundance, inexpensive and offer high adsorption capacity (Koohsaryan and Anbia 2016; Misaelides 2011). However, despite the advantages of zeolites, their limitation includes difficult separation from solution and a reduction in surface area due to agglomeration when mass is increased (Putra and Lee 2020). Therefore, adding zeolite to chitosan to form a composite material is postulated to improve the resulting adsorbent's mechanical and thermal stability. The present study explored the separation of the adsorbent from water by incorporating iron oxide (Fe_3O_4), which became helpful for the regeneration and reusability of the adsorbent.

Therefore, the present study aimed to incorporate three materials; chitosan, zeolite, and iron oxide for the synthesis of a magnetic composite. The synthesised composite was used as an adsorbent in an ultrasound-assisted magnetic solid-phase extraction (UA-MSPE) of TCs in wastewater and river water samples. In this regard, chitosan acted as a cation favourable for the adsorption of anionic TC species. In contrast, excess negative charge on the surface of zeolites (Makgabutlane et al. 2020; Margeta et al. 2013) makes them advantageous for the adsorption of cationic TC species, with iron oxide introducing the magnetic properties in the resulting composite. Upon efficient extraction and pre-concentration process, a high performance liquid chromatography equipped with a photodiode array detector (HPLC-DAD) was used for the quantification of all the investigated TCs.

Materials and methods
Chemicals
All reagents procured for the present study were of analytical grade and used without further purification. Ultrapure water (18 MΩ cm^{-1} resistivity, Millipore, Bedford, MA, USA) was used to prepare all water-based solutions. Tetracycline (98–102%), oxytetracycline dehydrate (95–102%), doxycycline monohydrate (purity not indicated by supplier), iron (II) tetrahydrate ($FeCl_2·4H_2O$), zeolite, chitosan, sodium hydroxide (NaOH), hydrochloric acid (HCl), iron (III) chloride hexahydrate ($FeCl_3·6H_2O$), oxalic acid dihydrate (OA), acetic acid (99%) and HPLC-grade solvents (acetonitrile (ACN) and methanol (MeOH)) were procured from Sigma Aldrich (St. Loius, MO, USA).

Synthesis of chitosan-Fe₃O₄ composites
The composite was synthesised by dispersing 1 g of chitosan in an acetic acid solution (0.25% v/v). To the chitosan solution, 30 mM of $FeCl_3·6H_2O$ and 15 mM of $FeCl_2·4H_2O$ were added, followed by stirring at 40 °C for 1 h under a nitrogen atmosphere. After that, 10% NaOH was added dropwise under vigorous stirring (700 rpm) until the solution pH reached 10. The resulting solution was further stirred for 1 h. The brown precipitate was collected using a magnet and washed several times with methanol and water, followed by drying in a 60 °C oven for 12 h. The same procedure was followed when preparing the Fe_3O_4, except that Cs were not added.

Preparation of chitosan-zeolite-Fe₃O₄ composites
Magnetic chitosan-zeolite ($Cs–Z–Fe_3O_4$) composites were prepared by adding 1 g of magnetic chitosan and 1 g of zeolite powder in acetic acid solution (5% v/v) under vigorous stirring (700 rpm) for 24 h at room temperature. After 24 h, the solution was sonicated for 30 min

to ensure equal distribution of zeolite particles into the magnetic chitosan solution. The resulting solution was centrifuged, and the concentrate was washed several times with water and dried at 60 °C for 24 h. The details of the analytical techniques used to characterise the materials are presented in the Additional file 1: Sect. SI 1.1.

Optimisation of UA-MSPE method

The selection of the suitable adsorbent and desorption solvent was optimised using a one-fact-at-a-time approach, and the methods used are described in the Additional file 1 (Sections SI 1.2 and SI 1.3). In addition, TCs were analysed with the HPLC-DAD system as described in the Additional file 1: Sect. SI 1.4. Tetracyclines were analysed with the HPLC-DAD system as described in the Additional file 1 (Section SI 1.4). Optimisation of the proposed sample preparation method is important to determine the best extraction and pre-concentration conditions to attain satisfactory results. In this study, a design of experiment approach was performed to simultaneously investigate factors that affect the extraction and pre-concentration of analytes in water. Factors investigated in this study included the mass of the adsorbent (MA), sample pH (pH), sample volume (SV), extraction time (EXT), eluent volume (EV) and elution time (ET). These factors were first screened using the two-level fractional factorial design (2^{6-2}), as shown in Additional file 1: Table S1. A total of 20 experiments were performed (Additional file 1: Table S2), and the results obtained were used further in the optimisation step.

Central composite design (CCD) was used to optimise the experimental conditions. Factors significant for the extraction process were optimised using the CCD, while others (not significant) were kept constant. A STATISTICA software (version 14) was used, and 18 experiments were generated (Additional file 1: Table S3). The low (−1), central (0) and high (+1) points for each factor are shown in Additional file 1: Table S4. The significance of each factor and the estimation of the goodness of fit in each experiment were achieved using variance analysis (ANOVA).

Adsorption studies

This step was essential for investigating the ability of the synthesised adsorbent to extract TCs in water. Therefore, adsorption studies were carried out by first preparing standard solutions of TCs in water with concentrations ranging from 2 to 20 mg L^{-1} in amber bottles, then adjusting the pH to a desired value. Afterwards, an appropriate amount of the adsorbent was added to each solution (250 mL). The mixture was then sonicated for 15 min, followed by the removal of the adsorbent with an

external magnet. The supernatant was filtered and analysed with HPLC-DAD. The adsorption capacity of each tetracycline antibiotic was calculated using Eq. (1):

$$q_e = \left(\frac{C_0 - C_e}{m} \right) V \tag{1}$$

where q_e, C_0, C_e, V and m are the equilibrium adsorption amounts of TCs on Cs–Z–Fe_3O_4 composite (mg g^{-1}), initial concentration of adsorbate (mg L^{-1}), equilibrium concentration of adsorbate (mg L^{-1}) volume of TC solution (L) and mass (g) of Cs–Z–Fe_3O_4, respectively.

Analysis of real samples

The developed and optimised analytical method was applied to analyse wastewater (influent and effluent) and surface water samples. Wastewater samples were sourced from the Babelegi wastewater treatment plant (WWTP) in Pretoria, South Africa (GPS coordinate: 25.35162° S, 28.27225° E). Surface water was collected from Apies River, flowing in Pretoria (GPS coordinate: 25.7268° S, 28.1715° E). The physicochemical properties of the water samples are presented in Additional file 1: Table S5. To the best of our knowledge, no previous studies have investigated the impact of pharmaceuticals on Babelegi WWTP.

In contrast, several pharmaceuticals are present in Apies River (Mhuka et al. 2020). Water was collected and stored in pre-cleaned Schott bottles in both study sites. Preservation was carried out by transporting samples into the laboratory while kept in cooler boxes filled with ice cubes. Samples were further preserved in the refrigerator set at 4 °C when not being treated for analysis. Sample preparation was performed by adding 58 mg of the adsorbent into 30 mL of each water sample. Ultrasonication was performed for 15 min, and then separating the adsorbent from the sample solution with an external magnet. Thereafter, desorption of analytes through sonication in a mixture of ACN and 0.01 M OA (20:80 v/v) for 15 min was performed. Before HPLC-DAD analysis, the extract was filtered through a 0.22 μm PVDF filter.

Regeneration and reusability of the synthesised adsorbent

Adsorption and desorption experiments were conducted using the optimised analytical method. This was necessary for investigating the ability to regenerate and reuse the synthesised adsorbent. Initially, 58 mg of the adsorbent was added to 30 mL of the model solution containing analytes at optimum pH of 7.00 and sonicated for 15 min. The adsorbent and supernatant were separated magnetically, and the supernatant was discarded. Desorption of analytes was achieved through sonication with ACN and 0.01 M OA (20:80 v/v) for 15 min to elute the

Lefatle *et al. Journal of Analytical Science and Technology*   (2023) 14:28

Page 4 of 15

adsorbed TCs from the adsorbent. Separation was performed using an external magnet, and the eluent was filtered through a 0.22 μm PVDF filter and analysed with HPLC-DAD. Subsequently, the adsorbent was rinsed with ultrapure water and dried at 60 °C overnight. Postdrying, the adsorbent was reused for the next adsorption and desorption cycle.

Results and discussion

FTIR analysis

The FTIR spectra of materials, chitosan (Cs-Neat), zeolite (Z-Neat) and iron oxide (Fe_3O_4-Neat) analysed before the synthesis of the composite (Cs–Z–Fe_3O_4), as well as the adsorbent itself, are given in Fig. 1. Based on the provided spectrum (Fig. 1a), the bands; 3395, 2864, 1640, 1555, 1378 and 1053 cm^{-1} were assigned to the characteristics functional groups of chitosan (Branca et al. 2016; Lustriane et al. 2018; Usman et al. 2012). The

zeolite spectrum (Fig. 1b) showed characteristic peaks at 3451 and 1665 cm^{-1}, which are attributed to the OH stretching and bending (Aloulou et al. 2017). The peaks at 990 cm^{-1} correspond to the Si–O–Al asymmetric stretching of T-O bonds (T represents Si or Al bonded tetrahedrally) (Abidin et al. 2017). Characteristic peaks at 665, 554 and 463 cm^{-1} were due to the Si–O–Si symmetric stretching and symmetric stretching of the double six-membered rings of the T–O–T and T–O symmetric bending, respectively (Abidin et al. 2017). In Fig. 1c, the presence of the bands at 3310, 2956, 2857, 1625 and 607/423 cm^{-1} were ascribed to O–H/N–H, C–H, C=O and Fe–O stretching vibration, respectively, which confirmed the formation of magnetic chitosan (Dadhore et al. 2018; Sharma & Jeevanandam 2013; Subadra et al. 2019; Shukla et al. 2015; Silva et al. 2013). The Cs–Z–Fe_3O_4 composite spectra showed characteristic peaks of Cs, Z and Fe_3O_4. The peak at 3434 cm^{-1} was attributed to
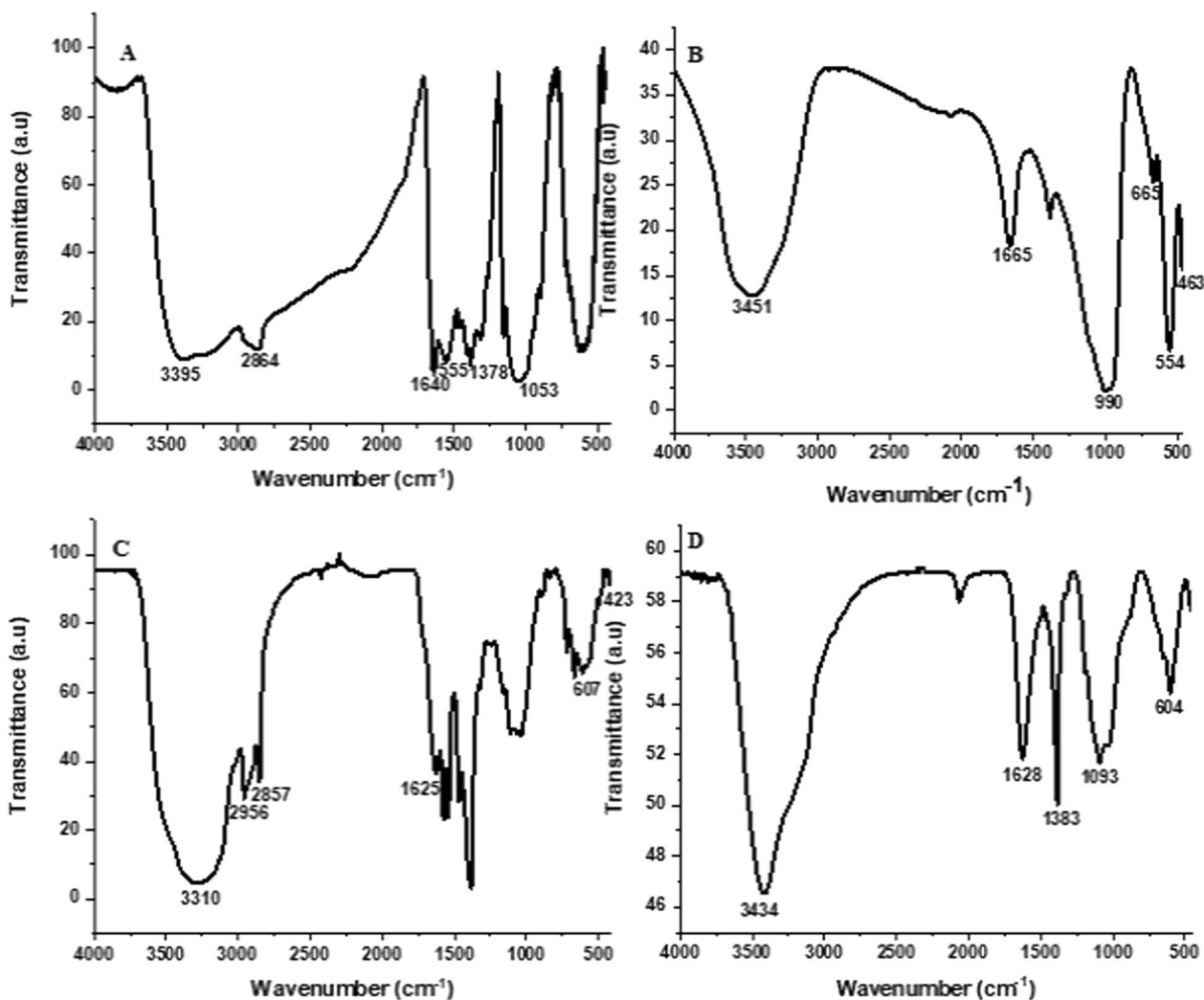

Fig. 1 FTIR spectra of **a** Cs-Neat, **b** Z-Neat, **c** Fe_3O_4-chitosan and **d** Cs–Z–Fe_3O_4 composite

the OH stretching vibrations from Cs, Z and Fe_3O_4. The 1628 and 1383 cm^{-1} peaks were due to the N–H stretching and C-H bending vibrations of the Cs, respectively. The peak at 1093 cm^{-1} represented the Si–O–Al stretching vibrations of T–O bonds from the Z. The peak at 604 cm^{-1} corresponds to the Fe–O stretching vibrations of the Fe_3O_4. From the results obtained it is evident that the composite was successfully prepared.

XRD analysis

The XRD patterns of Cs, Z (JCPDS card number 01-075-1151), Fe_3O_4 (JCPDS card number 04-013-9809), and Cs–Z–Fe_3O_4 composite are shown in Fig. 2. In Fig. 2a, the observed peaks at angles 10.2° and 20.0° corresponded to the crystalline nature of chitosan (Aziz et al. 2019). Furthermore, a peak at 41.1° was observed, ascribed to the amorphous nature of the biopolymer (Aziz et al. 2020).

The characteristic peaks associated with zeolite are seen at angles 7.2°,10.2°, 12.4°, 21.7°, 24.1°, 27.1°, 29.9°, 34.2° and 41.6° and the peaks were indexed to (1 0 0), (1 1 0), (1 1 1), (3 0 0), (3 1 1), (3 2 1), (4 1 0), (3 3 2) and (4 4 0), respectively. The characteristic peaks observed for iron oxide in magnetic chitosan (Fig. 2c) were in agreement with previous studies (Namvari & Namazi 2014; Swanson et al. 1967). The XRD pattern of the Cs–Z–Fe_3O_4 composite displayed decreased intensity of some zeolite and iron oxide peaks. All the peaks associated with Fe_3O_4 were present in the Cs–Z–Fe_3O_4 spectrum. However, only one peak ($2\theta = 10.2°$) from the Cs was visible, while only four peaks ($2\theta = 7.0°$, 10.2°, 24.0° and 27.0°) from the Z were visible. This suggested a change in the crystal structure of zeolite due to its interaction with chitosan (Abukhadra et al. 2021). The introduction of Z and Fe_3O_4 into the Cs matrix decreased the crystalline domain of Cs since the peak intensity of Cs in the composite was
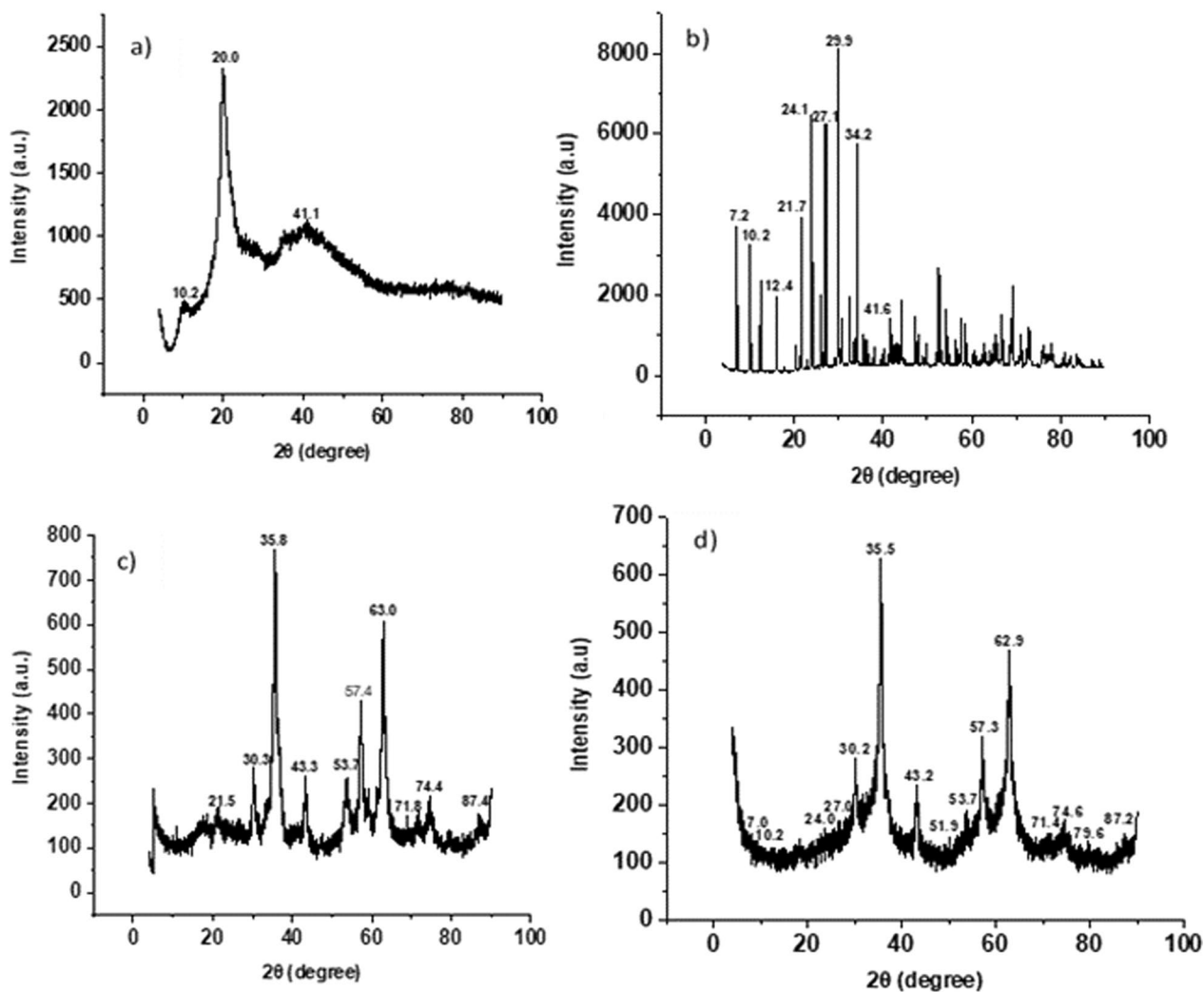

Fig. 2 XRD patterns of a Cs, **b** Z, **c** Fe_3O_4-chitosan and **d** Cs–Z–Fe_3O_4 composite

Lefatle *et al. Journal of Analytical Science and Technology*   (2023) 14:28

Page 6 of 15

weaker than that of the pure Cs. Therefore, as observed in Fig. 2d, a new composite material was successfully synthesised from Cs, Z and Fe_3O_4.

Morphological and elemental analysis

Transmission electron microscopy (TEM) images showed that the Fe_3O_4 nanoparticles (Fig. 3a) consisted of agglomerates of particles. These agglomerates could be ascribed to the large surface area to volume ratio and magnetic dipole–dipole interactions between the nanoparticles (Yu et al. 2011). As shown in Fig. 3a, the nanoparticles had different shapes dominated by spherical particles. The TEM image of Cs–Z–Fe_3O_4 composite is shown in Fig. 3b. The image showed that the Fe_3O_4 nanoparticles were successfully incorporated and dispersed in the chitosan and zeolite. The morphology of Cs, Z and the synthesised Fe_3O_4 and composite were analysed using SEM and the images obtained are presented in Fig. 3c–f. The SEM images of Cs showed lamellar structures, while the SEM image for Z and Fe_3O_4 showed particle-like structures. The composite exhibited aggregated granular shapes of the particles because of the presence of zeolite and iron oxide.

The EDS analysis of Cs, Z, Fe_3O_4 and Cs–Z–Fe_3O_4 composite are presented in Additional file 1: Fig. S1. The EDS of Cs only displayed the presence of C (56.8%) and O (43.2%). The absence of nitrogen in EDS results could be due to the absorption of Kalpha X-rays from the nitrogen in the chitosan sample by the beryllium window that separates the sample chamber from the analyser. In addition, due to its low-Z number, the nitrogen position may have laid between the C and O K-alpha, making it hard to quantify. EDS for Z showed the presence of O (44.8%), Si (20.1%), Al (19.7%), Na (15.4) and K (0.1%). EDS for Fe_3O_4 showed the presence of Fe (78.5%) and O (21.5%). The EDS analysis of the composite depicted two prominent peaks for Cs, which corresponded to C (10.9%) and O (27.7%). The peaks of O (27.7%), Si (6.5%) and Al (0.9%) were characteristic elements for Z. Furthermore, the presence of Fe (53.9%) confirmed the incorporation of Fe_3O_4.

Choice of an adsorbent

The best adsorbent for extracting and pre-concentrating TCs from an aqueous solution was investigated. This was done by synthesising a magnetic chitosan-zeolite composite, followed by its investigation for extracting and pre-concentrating TCs in water. In the same context, individual materials (i.e., chitosan, zeolite and iron oxide) used to synthesise the composite were investigated for their ability to extract TCs from water. All experiments were conducted in triplicate under the same experimental conditions. The results are presented in Additional file 1: Fig. S2. Due to high extraction recoveries, the composite proved to have an excellent ability to extract TCs from aqueous solutions than its counterparts. This is attributed to functional groups such as the amine and hydroxyl from the Cs and the high porosity and increased surface charge of the zeolite. In addition, combining the two materials (Cs and zeolite) into a composite resulted in enhanced extraction efficiency due to combining their individual properties. Secondly, textural properties such as surface area and porosity of an adsorbent play an important role in the extraction of contaminants from complex matrices. These two properties are crucial since they are strongly related to the adsorption capacity of an adsorbent (Carvalho et al. 2019). Therefore, the higher extraction efficiency observed for the composite could suggest that the composite had a higher surface area compared to the individual components.

Choice of desorption solvent

The selection of a suitable eluent is one of the most crucial factors when developing a method for UA-MSPE since it allows for satisfactory desorption of the desired analyte(s). The choice of eluent is based on the physicochemical properties of the desired analyte(s) and adsorbent and the chromatographic approach utilised for the analysis of target compounds. The eluent should be compatible with commonly used liquid chromatographic mobile phases. This study investigated four common solvents, acetonitrile, methanol, isopropanol, and oxalic acid, and their mixtures for eluting the adsorbed compounds. The results attained are shown in Additional file 1: Fig. S3. A combination of ACN and 0.01 M OA was the most effective eluent for removing all three TCs. The addition of oxalic acid significantly improved the extraction and pre-concentration of the TCs. This was due to the influence of pH changes on the physicochemical properties of the analytes and the adsorbent. This means the variation of sample pH alters the adsorbent surface charge and the chemical properties of TCs. Therefore, oxalic acid could promote the electrostatic repulsion between the protonated TCs and the positively charged adsorbent. On the other hand, the presence of ACN accelerated desorption due to its high permeability, thus facilitating the desorption of the TCs.

Optimisation of the sample preparation process
Fractional factorial design

Selective extraction and pre-concentration of the desired analyte(s) can be affected by several factors. However, not all factors may significantly affect the desired response during the extraction and pre-concentration process. Therefore, a two-level fractional factorial design is useful for screening factors that may have significant effects.
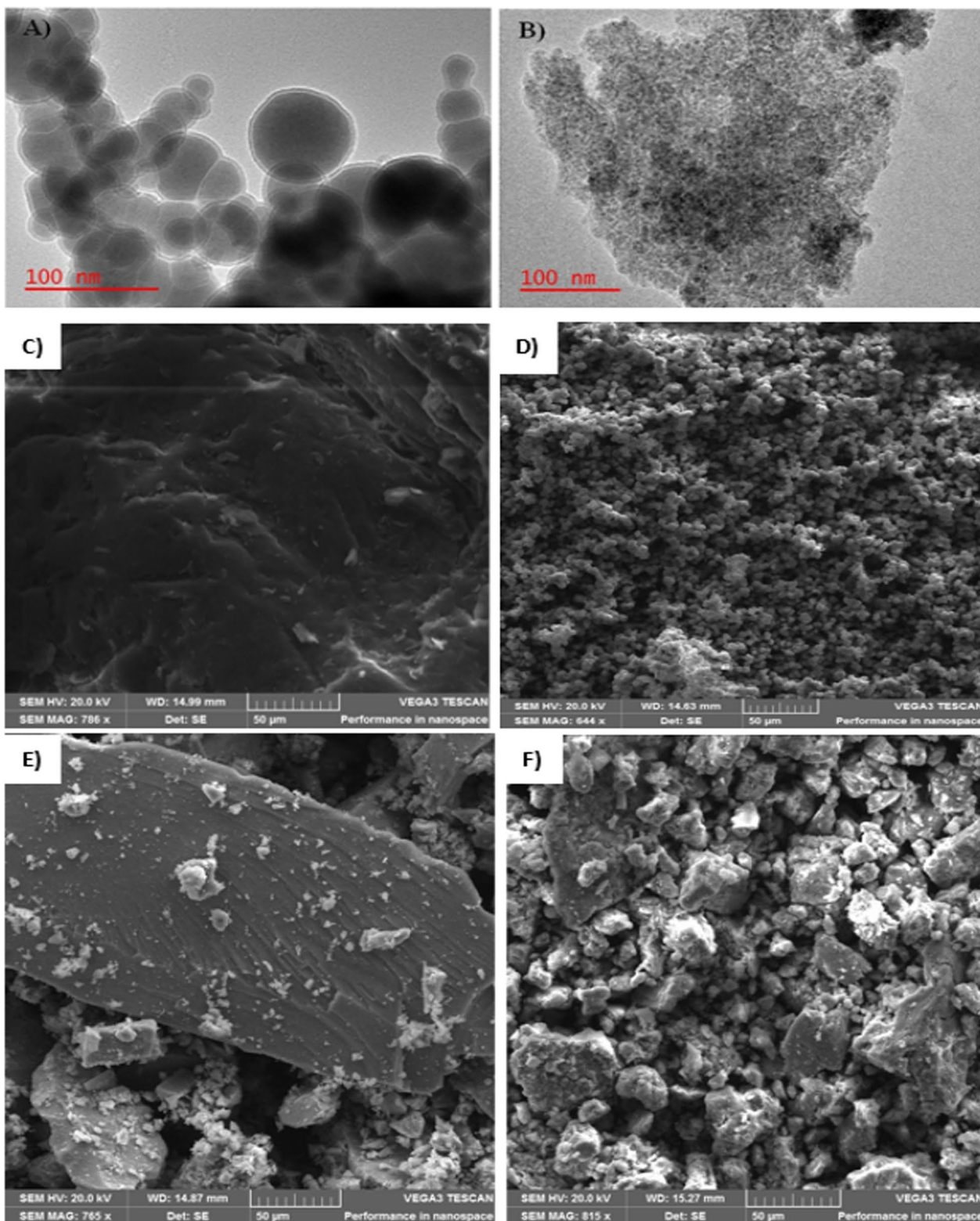
Lefatle *et al. Journal of Analytical Science and Technology* (2023) 14:28

Page 7 of 15

Fig. 3 TEM image of **A** Neat Fe_3O_4, and **B** chitosan-zeolite-Fe_3O_4 composite, SEM image of **C** Cs, **D** Zeolite, **E** Fe_3O_4 and **F** Cs–Z–Fe_3O_4 composite

Lefatle *et al. Journal of Analytical Science and Technology*   (2023) 14:28

Page 8 of 15

A 2^{6-2} fractional factorial design was employed and the results for each experiment are given in Additional file 1: Table S2. The analysis of variance (ANOVA) was used to investigate significant parameters, and the ANOVA results were visualised in a form of Pareto charts as shown in Additional file 1: Fig. S4. These results illustrate that elution volume (EV) and adsorbent mass (MA) were significant for extracting all three TCs. The duration of the extraction process (EXT) was only significant for oxytetracycline and doxycycline, while sample pH was significant only for doxycycline. Therefore, the pH of aqueous solution, adsorbent mass and extraction volume were optimised using the CCD.

Response surface methodology (RSM)

The RSM based on the CCD was utilised to optimise the extraction conditions and the 3D surface plots are shown in Fig. 4. The interactive effects of MA and pH showed that the concentration of TCs increased when mass was between 10 and 70 mg. An increase could have

influenced this in the availability of the adsorbent active/binding sites. The characterisation results have already indicated the presence of both hydroxyl and amino functional groups (Fig. 1) on the adsorbent surface which could serve as binding sites for TCs.

An increase in concentration was observed when the sample pH was between 4.5 and 8. The point of zero charge (pH_{pzc}) of the adsorbent was 4.20 (Additional file 1: Fig. S5), indicating that when the sample pH was below the pH_{pzc}, the surface of the adsorbent was positive and conversely, when the sample pH was above the pH_{pzc}, the surface of the adsorbent was negative. Tetracyclines tend to be cationic when the pH is less than 3.3, zwitterionic in pH range of 3.3–7.7 and anionic when pH is greater than 7.7. Between the pH of 4.5 and 8, electrostatic interactions are expected to occur between the negatively charged surface of the adsorbent and the zwitterionic species of the TCs which results in the increased concentration of TCs observed. Additionally, the effects of eluent volume were investigated. The results suggested
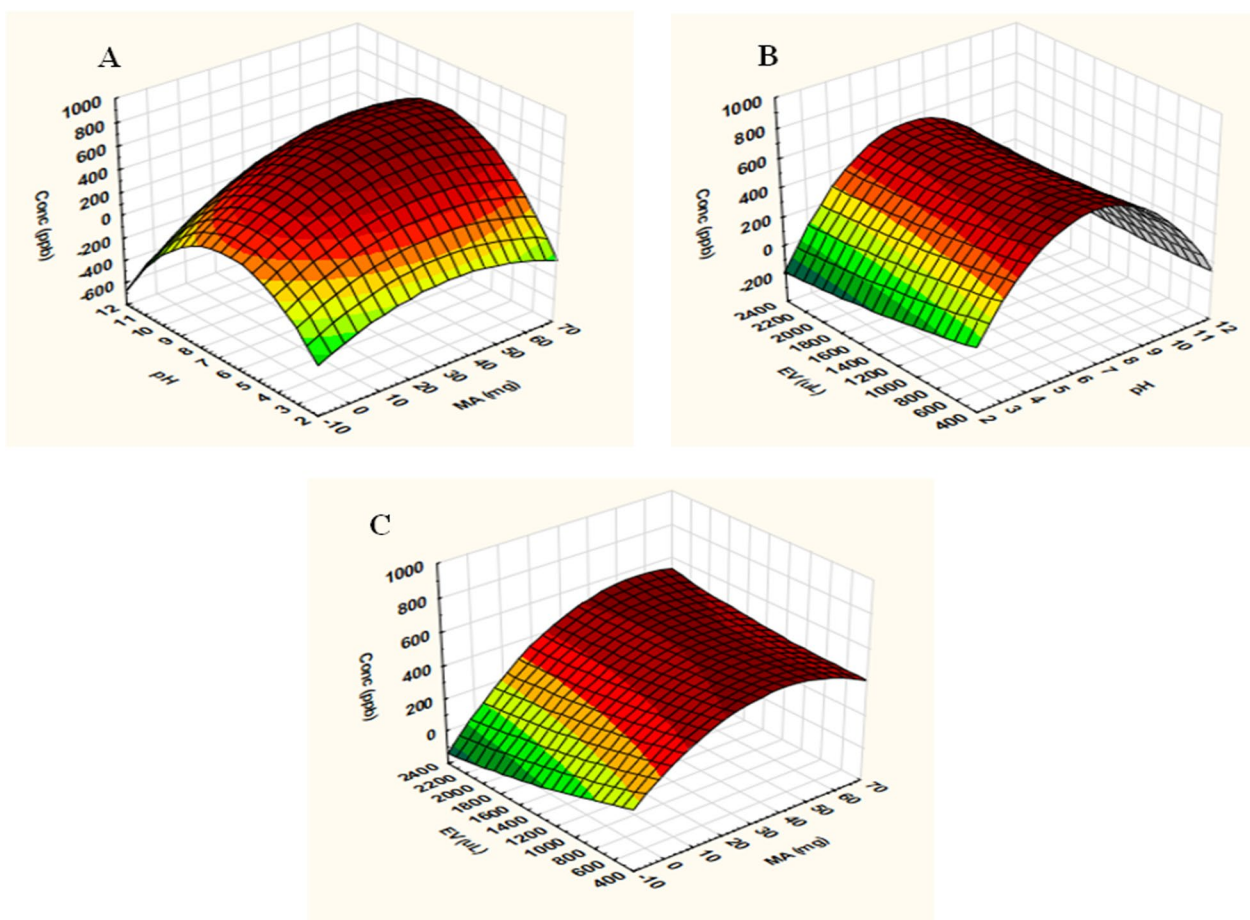

Fig. 4 Response surface plots illustrating interaction effects of **A** mass of adsorbent and sample pH, **B** sample pH and eluent volume and **C** mass of adsorbent and eluent volume on the concentration

Lefatle *et al. Journal of Analytical Science and Technology*   (2023) 14:28

Page 9 of 15

that the concentration increased with increasing eluent volume. This could be attributed to an increase in EV which increases desorption efficiency.

Desirability function

The estimation of optimum conditions, in addition to the 3D surface plots, was further investigated by using the profile for predicted values and desirability (Additional file 1: Fig. 5). From Fig. 5, maximum concentrations (464.9 µg L^{-1}) were assigned the desirability of 1, middle concentrations (274.6 µg L^{-1}) were assigned desirability of 0.5 and minimum concentrations (108.6 µg L^{-1}) were assigned desirability of 0. The desirability value of 1 was selected to attain optimum parameters. The results show that the optimum conditions for the pre-concentration of TCs were mass of adsorbent: 58 mg, sample pH: 9.12 and eluent volume: 2248.5 µL. However, a sample pH of 7 was used in further experiments since it was still within the desirability value of 1, with a probability to enhance the formation of zwitterionic forms of TCs. Therefore, the overall optimum conditions employed for the extraction and pre-concentration of TCs were 58 mg, 7.00, 30 mL, 15 min, 2248.5 µL and 15 min for MA, pH, SV, EXT, EV and ET, respectively. The obtained optimal parameters were verified experimentally. The obtained experimental

concentrations were 456.6 ± 4.11, 542.6 ± 10.70 and 433.6 ± 24.59 µg L^{-1} for OT, TC and DC, respectively. These results agreed with the RSM predicted values (464.9, 546.3 and 431.3 µg L^{-1} for OT, TC and DC, respectively). Therefore, the RSM model was considered an accurate method for optimising pre-concentration.

Adsorption isotherms

Adsorption isotherms provide information about the concentration of the analyte and the degree to which it accumulates on the surface of the adsorbent. The Langmuir, Freundlich and Sips models were utilised to obtain the adsorption isotherms. Additional file 1: Table S6 shows the linear equations and parameters calculated from the isotherm plots. The results show that Langmuir, Freundlich and Sips isotherm models yielded correlation coefficients (R^2) greater than 0.99, which suggests their adequacy in predicting the experimental data. However, it is observed that both Langmuir and Sips isotherm models best described the adsorption of OT, TC and DC onto the composite since they had the highest R^2 value compared to the Freundlich isotherm model. Based on the Langmuir isotherm, the results indicate that the adsorption of the three analytes onto Cs–Z–Fe$_3$O$_4$ occurred homogeneously with the formation of a
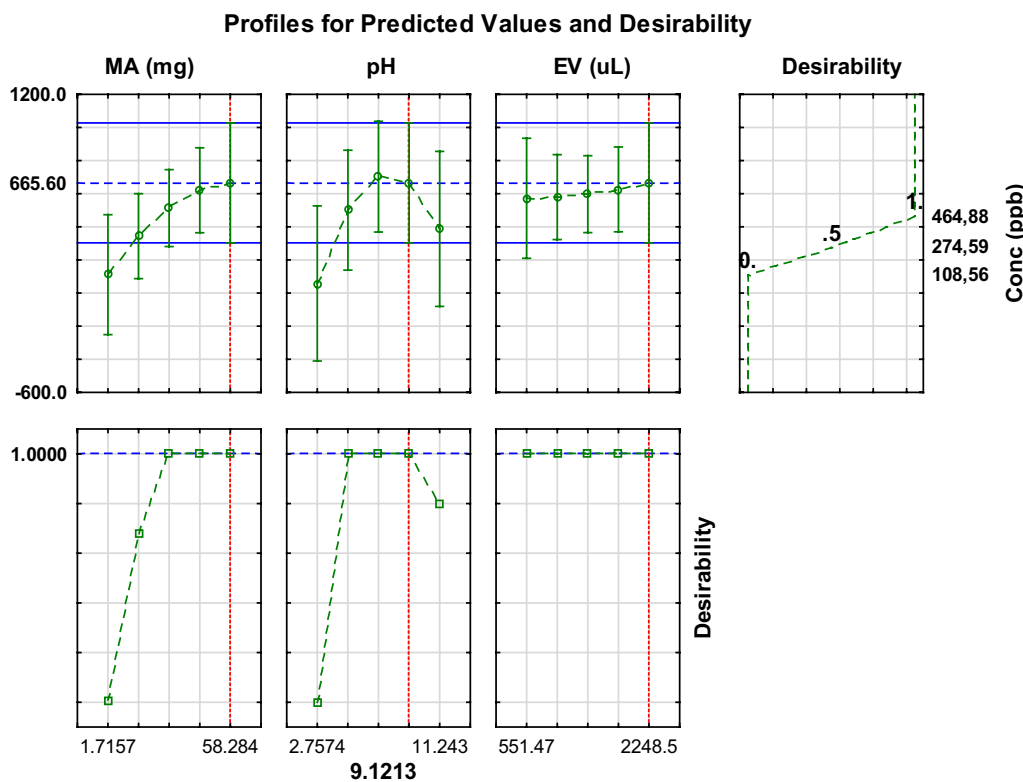

Fig. 5 Desirability function for pre-concentration of OT and its predicted maximum concentration

monolayer. The Sips isotherm model further validated the results obtained in the Langmuir isotherm model. The Sips equation consists of a dimensionless heterogeneity factor (n) that can be used to define the heterogeneity of the system when n is between 0 and 1. When $n = 1$, adsorption reduces to the Langmuir model; when $n > 1$, adsorption reduces to the Freundlich model (Vieira et al. 2018). The Sips isotherm model reduced to Langmuir isotherm since $n = 1$ for all three analytes suggesting homogeneous adsorption. From the Freundlich isotherm model, adsorption is favourable when $1 < n_f < 10$ (Alidadi et al. 2018). Even though the Freundlich model did not best fit the experimental data, it is worth noting that since $n_f > 1$ for all three analytes, this suggests that the adsorption was favourable.

Analytical performance

The analytical method validation was carried out as the International Conference on Harmonization (ICH) recommended. The analysis of OT, TC and DC using the UA-MSPE/HPLC-DAD was validated in terms of linearity, sensitivity (LOD and LOQ), specificity, robustness,

Table 1 Analytical performance of the UA-MSPE/ HPLC-DAD method

Parameters	OT	TC	DC
Linearity (µg L^{-1})	LOQ-400	LOQ-400	LOQ-400
R^2	0.9982	0.9985	0.9939
LOD (µg L^{-1})	0.05	0.35	0.67
LOQ (µg L^{-1})	0.14	1.05	2.03
Intraday (%RSD), $n = 4$	1.36	1.89	3.72
Interday (%RSD), $n = 3$	1.44	0.19	1.14
%ME	0.1	9.0	− 13.1

precision (repeatability and reproducibility), accuracy, and the matrix effect. The results are summarised in Table 1.

Linearity and sensitivity

Linearity was investigated by plotting the analyte concentration (LOQ-400 µg L^{-1}) against the analyte response from the analytical instrument. The results achieved good linearity for all analytes with correlation coefficients (R^2) exceeding 0.993. The sensitivity was measured using LOD (3.3 SD/m) and LOQ (10 SD/m). The SD values represented the standard deviations attained from 8 measurements ($n = 8$) of the lowest calibration standard solution, while m was the slope of the linear plot. The LODs for OT, TC and DC were found to be 0.05, 0.35 and 0.67 µg L^{-1}, respectively, while LOQs were 0.14, 1.05 and 2.03 µg L^{-1}, respectively.

Specificity

The specificity of the developed analytical approach was investigated by using the LC OpenLab software, and the results are shown in Fig. 6. The retention times of the analyte peaks for the spiked influent wastewater sample (Fig. 6b) and spiked ultrapure water (Fig. 6c) were similar. The standard deviation were 0.0085, 0.0099 and 0.0177 for OT, TC and DC, respectively.

Robustness

The developed method's robustness was determined by slight modifications on the injection volume, column temperature and flow rate as shown in Additional file 1: Table S7. The injection volume was changed from 20 to 15 µL and 25 µL, column temperature was changed from 25 to 22 °C and 28 °C, and the flow rate was changed from 1.00 to 0.97 mL min^{-1} and 1.03 mL min^{-1}. The
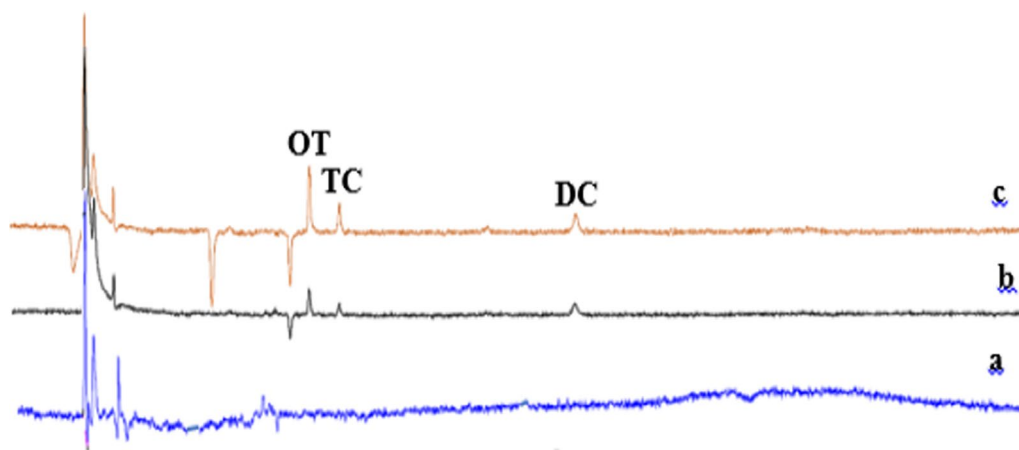

Fig. 6 Chromatograms of **a** blank, **b** spiked (100 ppb) influent wastewater sample and **c** spiked (100 ppb) Milli-Q water

robustness of the results is shown in Additional file 1: Table S7. From the low %RSD values, it can be deduced that the modification of the parameters had no significant effect on the peak areas with p values of 0.36, 0.43 and 0.76 for OT, TC and DC, respectively.

Precision and accuracy
Repeatability (intraday) and reproducibility (interday) of the developed method were reported in terms of the relative standard deviation (%RSD), and the results are shown in Table 1. All %RSD values were below 5%, which suggested that the proposed method has relatively good precision. The accuracy of the UA-MSPE/HPLC-DAD method was evaluated by spiking wastewater and river water samples. The data in Table 2 suggest that the recoveries for the three analytes represented an accurate analytical method with values above 90%.

Matrix effect
The matrix effect's influence on the analytical procedure's performance was assessed. The calibration curve method was used to investigate the matrix's effects. A calibration curve before and after pre-concentration was prepared, and slopes were determined. The percentage matrix effect (% ME) was calculated using Eq. (2) from the slopes.

$$\% \text{ ME} = \left(\frac{\text{Slope of matrix} - \text{Slope of solvent}}{\text{Slope of solvent}} \right) \times 100\% \tag{2}$$

According to literature, the matrix effect is categorised as having no effect when $\% \text{ ME} \geq -20\%$ or $\% \text{ ME} \leq 20\%$, medium when $-50\% \leq \% \text{ ME} \leq -20\%$ or $20\% \geq \%$ $\text{ME} \leq 50\%$, strong when $\% \text{ ME} \leq -50\%$ or $\% \text{ ME} \geq 50\%$ (Ferrer et al. 2011). The results showed that the % ME for OT, TC and DC were 0.1, 9.0 and -13.1. This suggested that all three TCs were not affected by the sample matrix effect, since $\%\text{ME} > -20$ for DC and $\%\text{ME} < 20$ for OT and TC.

Comparison of the proposed method with other studies
A comparison of the performance of the developed UA-MSPE/HPLC-DAD method with other published work was done. This was performed on the attained method validation parameters. Data used for comparison is presented in Additional file 1: Table S8. From Additional file 1: Table S8, it is observed that the developed UA-MSPE/HPLC-DAD method showed better LOD, LOQ and %RSD, indicating that it has better sensitivity and precision compared to the other published methods (Liu et al. 2014; Phiroonsoontorn et al. 2017; Sereshti et al. 2021b; Suarez et al. 2007; Yang et al. 2013). Therefore, the developed UA-MSPE/HPLC-DAD method can efficiently extract and pre-concentrate TCs in water.

Analysis of tetracyclines in wastewater and river water
The proposed UA-MSPE/HPLC-DAD experimental approach was used for the analysis of selected TCs in water samples. Results given in Table 2 indicate that none of the three analytes were found in water samples (Additional file 1: Fig. S3). The environmental water samples were spiked with the target compounds using different concentrations. This was necessary to establish if the applied analytical method could extract and detect the investigated compounds in real water samples. The results (Table 2) show that the analyte recoveries for OT,

Table 2 Validation of the UA-MSPE/HPLC-DAD method

Analytes	Added (µg L^{-1})	Influent		Effluent		River	
		Measured (µg L^{-1})	% R	Measured (µg L^{-1})	% R	Measured (µg L^{-1})	% R
Tetracyclines							
Oxytetracycline	0	–		–		–	
	5	4.61	92.2	4.77	95.4	4.79	95.7
	40	38.57	96.4	38.99	97.5	39.69	99.2
	100	98.64	98.6	99.92	99.9	100.54	100.5
Tetracycline	0	–		–		–	
	5	4.77	95.3	4.89	97.7	4.94	98.8
	40	38.86	97.2	39.39	98.5	39.86	99.7
	100	99.48	99.5	100.22	100.2	100.67	100.7
Doxycycline	0	–		–		–	
	5	4.52	90.3	4.58	91.5	4.59	91.8
	40	37.22	93.1	38.30	95.8	39.08	97.7
	100	96.61	96.6	98.27	98.3	98.83	98.8

TC and DC spiked at three different levels 92–101%, 95–101% and 90–99%, respectively. This means the applied analytical approach sufficiently extracted the target compounds from various sample matrices, followed by their analysis using HPLC-DAD, thus yielding accurate results. This further indicates that the proposed analytical method did not suffer from the sample matrix effects, with the attained results (Table 2) proving that the employed method is suitable for analysing the investigated drugs in real water samples.

Despite the non-detection of investigated compounds in the investigated water systems, tetracyclines have been previously found present in water samples across the world (Additional file 1: Table S9) (Abdallah et al. 2019; Hussain et al. 2016; Ibraheem & Abdul-Ahad 2012; Kanama et al. 2018; Mhuka et al. 2020; Monteiro et al. 2016; Ngumba et al. 2020; Sereshti et al. 2021a; Watkinson et al. 2009; Zhi et al. 2018). Additional file 1: Table S9 shows that a study by Hussain et al. 2016 showed the highest concentration of OT and DC, followed by previous studies by Hussain et al. (2016), Zhi et al. (2018). This was attributed to the presence of pharmaceutical companies in the study area with lack of water treatment facilities and the inefficiency of the wastewater treatment processes, respectively. Previous studies showed the highest concentrations of TC in influent wastewater with the observed concentrations of 45.4–54.4 µg L^{-1} (Kanama et al. 2018; Sereshti et al. 2021a). The results seen in the latter study were ascribed to the WWTP receiving wastewater from nearby hospitals. This means the concentrations detected in wastewater and river water samples are influenced by the surroundings, with pharmaceutical industries and hospitals playing a vital role. Hence, the present study presents a different scenario where the investigated compounds were not detected in the water systems. However, in the case of river water, the findings of the present study are similar to those reported in a different South African-based river (Mhuka et al. 2020).

Regeneration and reusability of the synthesised adsorbent

Regeneration and reusability of an adsorbent is important when considering real-world applications. Satisfactory reusability means that the adsorbent can be regenerated and used several times without the decrease in its adsorption capacity. As seen in Fig. 7, the percentage recovery decreased with each progressive cycle. The recovery for OT, TC and DC were below 70% after the ninth cycle. The reduction in percentage recovery could be ascribed to the decrease in the number of active binding sites on the surface of the Cs–Z–Fe$_3$O$_4$ composite. A study by Marotta et al. 2021 used chitosan/zeolite composite aerogel for the removal of indigo carmine and methylene blue dyes and the results showed that the recovery decreased to 60% after the adsorbent was used three times (Marotta et al. 2021). Additionally, chitosan/PVA/zeolite composite
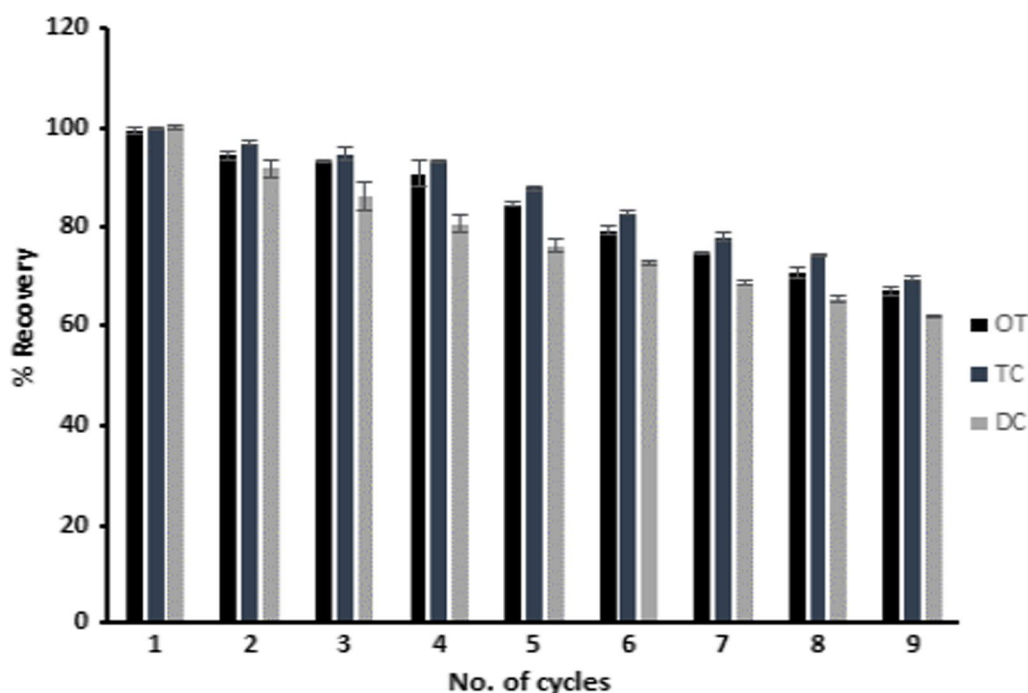

Fig. 7 The regeneration and reusability of Cs–Z–Fe$_3$O$_4$

membrane was used to remove Cr (VI), Fe (III) and Ni (II) ions by Habiba et al. (2017) and the adsorption capacity of the composite membrane decreased after the fifth cycle. Similar results were obtained by Gao et al. (2020) when chitosan/zeolite molecular sieves composite was used to remove nitrate (Gao et al. 2020). Therefore, the adsorbent showed satisfactory reusability and regeneration properties. The results indicate that Cs–Z–Fe_3O_4 composite is a promising adsorbent for extracting and pre-concentrating TCs in water.

Conclusion

In the current study, a magnetic chitosan-zeolite composite was synthesised successfully, confirmed by FTIR, XRD, SEM-EDS and TEM. The synthesised composite was successfully utilised as an adsorbent in an UA-MSPE for the simultaneous extraction and pre-concentration of OT, TC and DC in water. Parameters that affected the extraction and pre-concentration of the TCs such as mass of the adsorbent, sample pH, sample volume, extraction time, eluent volume and elution time, were investigated and optimised. The validated parameters under optimum conditions showed good linearity, sensitivity, precision and accuracy. Adsorption isotherms were best described by the Langmuir isotherm model suggesting a monolayer adsorption process, with the adsorption mechanism driven by electrostatic interactions. The proposed method was applied for the analysis of selected TCs in real samples, with none of the analytes detected in wastewater and river water. Finally, the prepared adsorbent showed good stability after several adsorption–desorption cycles.

Abbreviations

UA-MSPE	Ultrasound-assisted magnetic solid phase extraction
TCs	Tetracyclines
WWTP	Wastewater treatment plant
HPLC-DAD	High performance liquid chromatography equipped with a photodiode array detector
Cs	Chitosan
Z	Zeolite
Fe_3O_4	Iron oxide
MeOH	Methanol
ACN	Acetonitrile
OA	Oxalic acid dihydrate
CCD	Central composite design
MA	Mass of adsorbent
SV	Sample volume
EXT	Extraction time
EV	Extraction volume
ET	Elution time
FTIR	Fourier transform infrared
XRD	X-ray diffraction
SEM	Scanning electron microscopy
TEM	Transmission electron microscope
EDS	Energy dispersive X-ray spectroscopy

Supplementary Information

The online version contains supplementary material available at https://doi.org/10.1186/s40543-023-00394-1.

Additional file 1. Supplementary Information.

References
Abdallah M, Nguyen K, Ebele A, Atia N, Ali H, Harrad S. A single run, rapid polarity switching method for determination of 30 pharmaceuticals and personal care products in waste water using Q-Exactive Orbitrap high resolution accurate mass spectrometry. J Chromatogr A. 2019;1588:68–76.

Abidin A, Bakar A, Ng E, Tan W. Rapid degradation of methyl orange by Ag doped zeolite X in the presence of borohydride. J Taibah Univ Sci. 2017;11:1070–9.

Abukhadra M, Mostafa M, Jumah M, Al-Khalawi N, Alruhaimi R, Salama Y. Insight into the adsorption properties of chitosan/zeolite-A hybrid structure for effective decontamination of toxic Cd (II) and As (V) ions from the aqueous environments. J Polym Environ. 2021;30:295–307.

Alidadi H, Dolatabadi M, Davoudi M, Barjasteh-Askari F, Jamali-Behnam F, Hosseinzadeh A. Enhanced removal of tetracycline using modified sawdust: optimisation, isotherm, kinetics, and regeneration studies. Process Saf Environ Prot. 2018;117:51–60.

Aloulou H, Bouhamed H, Ghorbel A, Amar R, Khemakhem S. Desalination and water treatment elaboration and characterisation of ceramic microfiltration membranes from natural zeolite: application to the treatment of cuttlefish effluent. Desalin Water Treat. 2017;95:1–9.

Aziz S, Karim W, Brza M, Abdulwahid R, Saeed S, Al-Zangana S. Ion transport study in CS: POZ based polymer membrane electrolytes using trukhan model. Int J Mol Sci. 2019;20:1–20.

Aziz S, Marf A, Dannoun E, Brza M, Abdullah R. The study of the degree of crystallinity, electrical equivalent circuit, and dielectric properties of polyvinyl alcohol (PVA)-based biopolymer electrolytes. Polymers. 2020;12:1–17.

Branca C, D'Angelo G, Crupi C, Khouzami K, Rifici S, Ruello G. Role of the OH and NH vibrational groups in polysaccharide nanocomposite interactions: a FTIR-ATR study on chitosan and chitosan/clay films. Polymer. 2016;99:614–22.

Carvalho C, Rodrigues D, Lima É, Umpierres C, Chaguezac D, Machado F. Kinetic, equilibrium, and thermodynamic studies on the adsorption of ciprofloxacin by activated carbon produced from Jerivá (*Syagrus romanzoffiana*). Environ Sci Pollut Res. 2019;26:4690–702.

Dadhore H, Kaur C, Shrivastava S, Choudhary R (2018) Synthesis and characterisation of zero valent iron nanoparticles. Paper presented at the AIP Conference Proceedings 2100, Indore

deAlvarenga E. Characterization and properties of chitosan. In: Elnashar M, editor. Biotechnology of biopolymers. Rijeka: InTech; 2011. p. 91–108.

Elsoud M, Kady E. Current trends in fungal biosynthesis of chitin and chitosan. Bull Natl Res Cent. 2019;43:1–12.

Feria-Diaz J, Tavera-Quiroz M, Vergara-Suarez O. Efficiency of chitosan as a coagulant for wastewater from slaughter houses. Ind J Sci Technol. 2018;11:1–13.

Ferrer C, Lozano A, Agüera A, Girón A, Fernández-Alba A. Overcoming matrix effects using the dilution approach in multiresidue methods for fruits and vegetables. J Chromatogr A. 2011;1218:7634–9.

Gao Y, Bao S, Zhang L, Zhang L. Nitrate removal by using chitosan/zeolite molecular sieves composite at low temperature: characterisation, mechanism, and regeneration studies. Desalin Water Treat. 2020;203:160–71.

Habiba U, Afifi AM, Salleh A, Ang BC (2017) Chitosan/(polyvinyl alcohol)/zeolite electrospun composite nanofibrous membrane for adsorption of Cr6+ Fe3+ and Ni2+. J Hazard Mater 322:182–194. https://doi.org/10.1016/j.jhazmat.2016.06.028

Hussain S, Naeem M, Chaudhry M. Estimation of residual antibiotics in pharmaceutical effluents and their fate in affected areas. Pol J Environ Stud. 2016;25:607–14.

Ibraheem J, Abdul-Ahad M. Detection of tetracycline, doxycycline, chlortetracycline, and oxytetracycline antibiotics in Nineveha drug wastewater. NUCEJ. 2012;15:215–21.

Kanama K, Daso A, Mpenyana-Monyatsi L, Coetzee M. Assessment of pharmaceuticals, personal care products, and hormones in wastewater treatment plants receiving inflows from health facilities in North West Province, South Africa. J Toxicol. 2018;2018:1–16.

Koohsaryan E, Anbia M. Nanosized and hierarchical zeolites: a short review. Chin J Catal. 2016;37:447–67.

Liu M, Li Y, Lin S, Dong X. Determination of tetracycline residues in lake water by on-line coupling of molecularly imprinted solid phase extraction with high performance liquid chromatography. Anal Methods. 2014;6:9446–52.

Lodhi G, Kim Y, Hwang J, Kim S, Jeon Y, Je J, et al. Chitooligosaccharide and its derivatives: preparation and biological applications. Biomed Res Int. 2014;2014:1–13.

Lu Z, Peng J, Song M, Liu Y, Liu X, Huo P, et al. Improved recyclability and selectivity of environment-friendly MFA-based heterojunction imprinted photocatalyst for secondary pollution free tetracycline orientation degradation. Chem Eng J. 2019;360:1262–76.

Lustriane C, Dwivany F, Suendo V, Reza M. Effect of chitosan and chitosan-nanoparticles on post harvest quality of banana fruits. J Plant Biotechnol. 2018;45:36–44.

Madikizela L, Chimuka L. Occurrence of naproxen, ibuprofen, and diclofenac residues in wastewater and river water of KwaZulu-Natal Province in South Africa. Environ Monit Assess. 2017;189:1–12.

Makgabutlane B, Nthunya L, Musyoka N, Dladla B, Nxumalo E, Mhlanga S. Microwave-assisted synthesis of coal fly ash-based zeolites for removal of ammonium from urine. RSC Adv. 2020;10:2416–27.

Mamani M, Reyes F, Rath S. Multiresidue determination of tetracyclines, sulphonamides and chloramphenicol in bovine milk using HPLC-DAD. Food Chem. 2009;117:545–52.

Margeta K, Logar N, Siljeg M, Farkas M. Natural zeolites in water treatment—how effective is their use. In: Elshorbagy W, Chowdhury R, editors. water treatment. Rijeka: InTech; 2013. p. 81–112.

Marotta A, Luzzi E, deLuna M, Aprea P, Ambrogi V, Filippone G. Chitosan/zeolite composite aerogels for a fast and effective removal of both anionic and cationic dyes from water. Polymers. 2021;13:1–11.

Mhuka V, Dube S, Nindi M. Occurrence of pharmaceutical and personal care products (PPCPs) in wastewater and receiving waters in South Africa using LC-Orbitrap™ MS. Emerg Contam. 2020;6:250–8.

Minale M, Gu Z, Guadie A, Kabtamu D, Li Y, Wang X. Application of graphene-based materials for removal of tetracyclines using adsorption and photocatalytic-degradation: a review. J Environ Mana. 2020;276:1–19.

Misaelides P. Application of natural zeolites in environmental remediation: a short review. Microporous Mesoporous Mater. 2011;2011(144):15–8.

Monteiro M, Spisso B, dosSantos J, daCosta R, Ferreira R, Pereira M. Occurrence of antimicrobials in river water samples from rural region of the State of Rio de Janeiro, Brazil. J Environ Prot. 2016;7:230–41.

Namvari M, Namazi H. Clicking graphene oxide and Fe$_3$O$_4$ nanoparticles together: an efficient adsorbent to remove dyes from aqueous solutions. Int J Environ Sci Technol. 2014;11:1527–36.

Ngumba E, Gachanja A, Nyirenda J, Maldonado J, Tuhkanen T. Occurrence of antibiotics and antiretroviral drugs in source-separated urine, groundwater, surface water and wastewater in the peri-urban area of Chunga in Lusaka. Zambia Water SA. 2020;46:278–84.

Önal A. Overview on liquid chromatographic analysis of tetracycline residues in food matrices. Food Chem. 2011;127:197–203.

Phiroonsoontorn N, Sansuk S, Santaladchaiyakit Y, Srijaranai S. The use of dissolvable layered double hydroxide components in an in situ solid-phase extraction for chromatographic determination of tetracyclines in water and milk samples. J Chromatogr A. 2017;1519:38–44.

Putra R, Lee Y. Entrapment of micro-sized zeolites in porous hydrogels: strategy to overcome drawbacks of zeolite particles and beads for adsorption of ammonium ions. Sep Purif Technol. 2020;237:1–8.

Qin Y, Li P, Guo Z. Cationic chitosan derivatives as potential antifungals: a review of structural optimisation and applications. Carbohyd Polym. 2020;236:1–17.

Sereshti H, Abdolhosseini G, Soltani S, Jamshidi F, Nouri N. Natural thymol-based ternary deep eutectic solvents: Application in air-bubble assisted-dispersive liquid-liquid microextraction for the analysis of tetracyclines in water. J Sep Sci. 2021a;44:3626–35.

Sereshti H, Karami F, Nouri N, Farahani A. Electrochemically controlled solid phase microextraction based on conductive polyaniline-graphene oxide nanocomposite for extraction of tetracyclines in milk and water. J Sci Food Agric. 2021b;101:2304–11.

Sharma G, Jeevanandam P. A facile synthesis of multifunctional Iron oxide@ Ag core–shell nanoparticles and their catalytic applications. Eur J Inorg Chem. 2013;2013:6126–36.

Shukla S, Arora V, Jadaun A, Kumar J, Singh N, Jain V. Magnetic removal of Entamoeba cysts from water using chitosan oligosaccharide-coated iron oxide nanoparticles. Int J Nanomedicine. 2015;10:4901–17.

Siddeeg S, Tahoon M, Mnif W, Rebah F. Iron oxide/chitosan magnetic nano-composite immobilised manganese peroxidase for decolorisation of textile wastewater. Processes. 2020;8:1–12.

Silva V, Andrade P, Silva M, Bustamante A, Valladares L, Aguiar J. Synthesis and characterisation of Fe$_3$O$_4$ nanoparticles coated with fucan polysaccharides. J Magn Magn Mater. 2013;343:138–43.

Suárez B, Santos B, Simonet BM, Cárdenas S, Valcárcel M. Solid-phase extraction-capillary electrophoresis-mass spectrometry for the determination of tetracyclines residues in surface water by using carbon nanotubes as sorbent material. J Chromatogr A. 2007;1175(1):127–32. https://doi.org/10.1016/j.chroma.2007.10.033

Subadra U, Sutiami R, Taufiq A, Diantoro M, Sunaryono T, Hidayat A. Preparation and characterisation of magnetite nanoparticles combined with polyaniline and activated carbon. IOP Conf Ser Earth Environ Sci. 2019;276:1–8.

Swanson H, McMurdie H, Morris M, Evans E. Standard X-ray diffraction powder patterns, vol. 25. Washington, DC: US Department of Commerce; 1967.

Usman M, Ibrahim N, Shameli K, Zainuddin N, Yunus W. Copper nanoparticles mediated by chitosan: synthesis and characterisation via chemical methods. Molecules. 2012;17:14928–36.

Vieira R, Vilela P, Becegato V, Paulino A. Chitosan-based hydrogel and chitosan/acid-activated montmorillonite composite hydrogel for the adsorption and removal of Pb^{+2} and Ni^{+2} ions accommodated in aqueous solutions. J Environ Chem Eng. 2018;6:2713–23.

Watkinson A, Murby E, Kolpin D, Costanzo S. The occurrence of antibiotics in an urban watershed: from wastewater to drinking water. Sci Total Environ. 2009;407:2711–23.

Xiong W, Zeng Z, Li X, Zeng G, Xiao R, Yang Z, et al. Multi-walled carbon nanotube/amino-functionalised MIL-53(Fe) composites: remarkable

adsorptive removal of antibiotics from aqueous solutions. Chemosphere. 2018;210:1061–9.

Yan L, Liu Y, Zhang Y, Liu S, Wang C, Chen W, et al. $ZnCl_2$ modified biochar derived from aerobic granular sludge for developed microporosity and enhanced adsorption to tetracycline. Bioresour Technol. 2020;297:1–10.

Yang X, Yang C, Yan X. Zeolite imidazolate framework-8 as sorbent for on-line solid-phase extraction coupled with high-performance liquid chromatography for the determination of tetracyclines in water and milk samples. J Chromatogr A. 2013;1304:28–33.

Yu C, Gou L, Zhou X, Bao N, Gu H. Chitosan–Fe_3O_4 nanocomposite based electrochemical sensors for the determination of bisphenol A. Electrochim Acta. 2011;56:9056–63.

Zhi S, Zhou J, Yang F, Tian L, Zhang K. Systematic analysis of occurrence and variation tendency about 58 typical veterinary antibiotics during animal wastewater disposal processes in Tianjin, China. Ecotoxicol Environ Saf. 2018;165:376–85.

Publisher's Note